Intermetallics 33 (2013) 73–80

Contents lists available at SciVerse ScienceDirect

Intermetallics

journal homepage: www.elsevier.com/locate/intermet

Experimental investigation and thermodynamic optimization of the Al–Zn–Ti system in the Al-rich corner

Qun Luo [a], Qian Li [a], Jie-Yu Zhang [a], Shuang-Lin Chen [a,b], Kuo-Chih Chou [a,*]

[a] Shanghai Key Laboratory of Modern Metallurgy & Materials Processing, Shanghai University, 149 Yanchang Road, Shanghai 200072, China
[b] CompuTherm, LLC, Madison, WI 53719, USA

ARTICLE INFO

Article history:
Received 12 June 2012
Received in revised form
30 August 2012
Accepted 25 September 2012
Available online 10 November 2012

Keywords:
A. Ternary alloy systems
B. Phase diagrams
E. Phase diagram, prediction

ABSTRACT

The phase relationships of the Al–Zn–Ti system in the Al-rich corner (up to 25 at.% Ti and 60 at.% Zn) at 500 °C and 400 °C were experimentally studied. The annealed samples were investigated by means of optical microscopy (OM), scanning electron microscopy (SEM), energy dispersive X-ray spectrometer (EDS) and X-ray powder diffraction (XRD). The experimental results showed that the ternary phase τ –$Ti_{25}Al_{75-x}Zn_x$ (x = 19–60) was stable in the temperature range of 400–500 °C. A new $Ti_{28}Al_{68}Zn_4$ phase different from $TiAl_3$ phase was in equilibrium with (Al) and τ in the Al-rich corner. Based on the isothermal experimental data at 500 °C and 400 °C, a set of self-consistent thermodynamic description of the Al–Zn–Ti system was obtained.

1. Introduction

The Zn–Al alloys are typically and extensively used as superplastic materials which have been popularly applied to engineering components and the automotive industry [1]. A fundamental requirement for superplasticity is that the grain size should be very small and typically less than ~10 μm [2–4]. Kawasaki et al. [2] and Hirata et al. [5] reported the superplasticity of the fine grained Zn–22 wt.%Al alloys was possibly applied to seismic dampers and incorporated in the structures of buildings to protect against earthquake damage [6]. Recently, grain refinement is widely used in Al–Zn alloys to improve the comprehensive mechanical property and wearing resistance. Ti can be used to refine the grains of aluminum foundries and Al–Zn alloy [7–9], and also improve plastic properties, strength [10,11], and damping properties of cast alloys [12,13]. However, the mechanism of grain refinement is still controversial. Zhang et al. [14] found that excellent atomic matching between $TiAl_3$ and primary Al. But Iqbal et al. [15] thought that the $TiAl_3$ phase was metastable at the titanium concentration below 0.15 wt.% in aluminum alloys.

The structure of the precipitated phases formed by adding Ti in the Al–Zn alloys and the phase equilibrium relationships of the Al–Zn–Ti system will help us understand the reason the addition of Ti could refine the grains of Al–Zn alloys. The crystal structure of the new τ–$Ti_{26}Al_{55}Zn_{19}$ had been analyzed in our previous work [16]. The phase equilibria of the Al–Zn–Ti system in the Al-rich corner at 400 °C had been experimentally investigated [17]. In this paper, we focus on experimental determination of the phase equilibria in the Al-rich corner at 500 °C and thermodynamical assessment of the Al–Zn–Ti system.

2. Review of the literature information

There are three binary subsystems in the Al–Zn–Ti system: Al–Zn, Al–Ti and Zn–Ti. The phase relationships of the Al–Zn system are relatively simple. There are only three stable solution phases in this system, i.e. the liquid, (Al) and (Zn) phases. The thermodynamic description on the Al–Zn system included in the framework of COST Action 507 as well as reported by Mey [18] was chosen in this work. For the Al–Ti system, the calculated phase diagram and the thermodynamic functions assessed by Zhang et al. [19] agreed well with the critically evaluated experimental data reported in literatures and was accepted in this work. Owing to the large difference between the high melting temperature of Ti (1670 °C) and the low boiling point of Zn (907 °C), only part of the phase equilibria of the Zn–Ti binary system [20,21] was deduced and the divergence on intermetallic phases in this system still have existed [22–25]. In our previous work [26], the Zn–Ti system was optimized based on the available experimental data [23,27] and the former thermodynamic evaluation [28].

* Corresponding author. Tel.: +86 21 56333853.
E-mail addresses: shukcc@126.com, kcc126@126.com (K.-C. Chou).

0966-9795/$ – see front matter © 2012 Elsevier Ltd. All rights reserved.
http://dx.doi.org/10.1016/j.intermet.2012.09.027

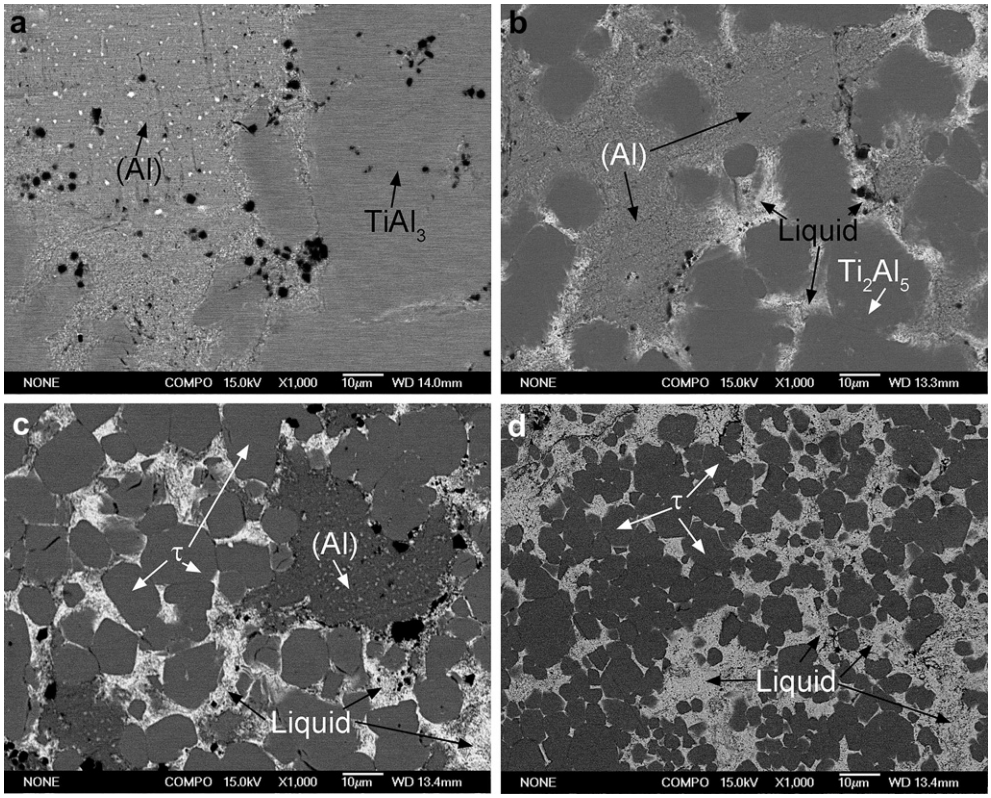

Fig. 1. The backscattered electron images of samples #1–#4 after annealing at 500 °C for 40 days: (a) the image of #1 sample, (b) the image of #2 sample, (c) the image of #3 sample, (d) the image of #4 sample.

Yang et al. [29] determined the phase relationships in the Zn-rich corner of the Zn–Al–Ti ternary system at 450 °C using equilibrated alloys and diffusion couple approach. The results revealed that the composition of the new phase τ is different from that of $TiAl_3$ phase and fluctuates in a relatively wide composition range of Zn from 11.6 to 58.4 at.%, Al from 14.8 to 59.8 at.% and Ti from 23.5 to 28.6 at.%, respectively. For the ternary phase, Raman and Schubert [30] synthesized $Al_{66}Zn_9Ti_{25}$ alloy by sintering pure Al, Ti and Zn powders and obtained a mixture of $D0_{22}$ and $L1_2$ phases. Krajewski [31] studied the atom site preference in $TiZn_3$-based trialuminides using H. Rietveld method, and found that Zn was replaced by Al during the transformation from $TiZn_3$ to $Ti(Al,Zn)_3$. In our previous work [16], the existence of the τ–$Ti_{26}Al_{55}Zn_{19}$ phase has been confirmed by Zn/$TiAl_3$ diffusion couple at 400 °C. The crystal structure and thermal stability of the τ–$Ti_{26}Al_{55}Zn_{19}$ alloy were experimentally determined. Then the phase equilibria of the Al–Zn–Ti system in Al-rich corner at 400 °C were experimentally investigated through equilibrated alloys [17]. Delsante et al. [27] measured the formation heat of alloys along the $TiZn_3$–$TiAl_3$ section at 27 °C using a high temperature direct drop calorimeter. Few thermodynamic assessments of the Al–Zn–Ti system had been reported except our previous work [26] which based on limited experimental data [27,29].

3. Experimental

The samples were prepared by sintering compacts which made from the elemental Al (99.5%, −325 mesh), Zn (99.5%, −325 mesh) and Ti (99.5%, −325 mesh) powders. The powders were weighted and ball milled in argon atmosphere. Then the mixed powders were pressed to obtain the pellets and then enclosed in corundum crucible by high temperature sealant. Those procedures were operated in a glove box with high pure argon to prevent the powders from oxidation. Each alloy was heated to 800 °C and kept for 24 h, then cooled in a chamber type electric resistance furnace to 500 °C. After homogenizing at 500 °C for 40 days, the samples were quenched in water. The $Ti_{25}Al_{75}$ and $Ti_{26.2}Al_{69.3}Zn_{4.5}$ alloys were prepared by mixing and sintering the elemental powders of Al, Zn and Ti at 800 °C for 24 h and cooled in furnace. Parts of $Ti_{26.2}Al_{69.3}Zn_{4.5}$ alloys were annealed at 500 °C for 5 days and quenched in water.

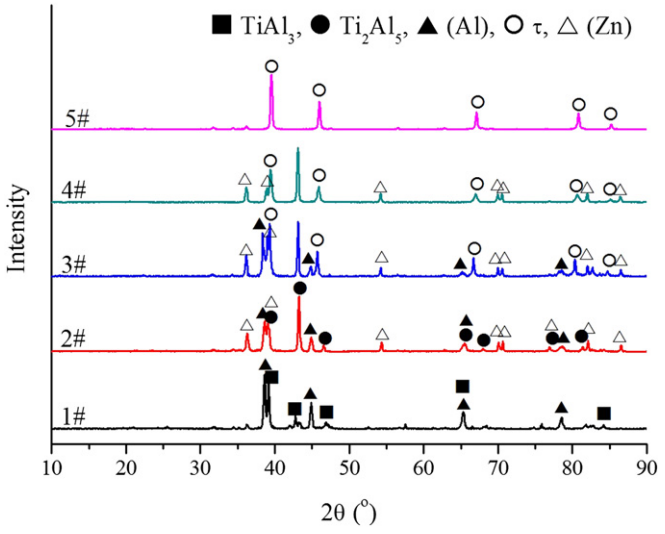

Fig. 2. The XRD patterns of samples #1–#5 after annealing at 500 °C for 40 days.

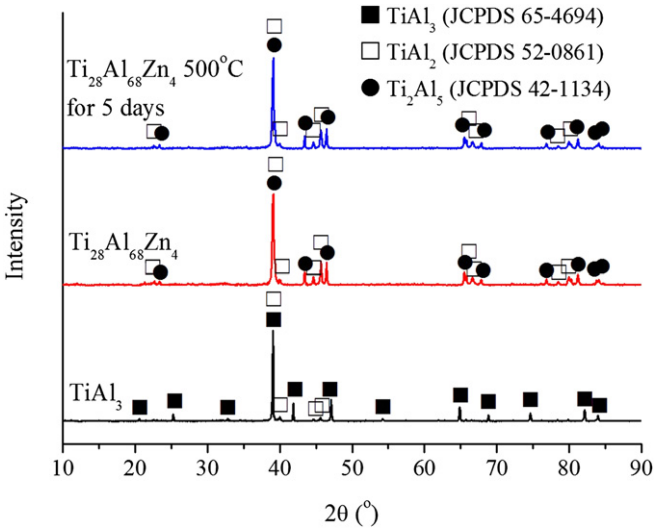

Fig. 3. The XRD patterns of $TiAl_3$ and $Ti_{28}Al_{68}Zn_4$ powders.

The composition of all samples was determined by inductively coupled plasma atomic emission spectrometry (ICP). XRD was used to analyze the phase compositions and structures. The microstructure investigations of etched samples were made by means of optical microscopy (OM), JSM–6700F SEM. The compositions of the various phases in samples were examined using EDS.

4. Results and discussions

Fig. 1 shows the backscattered electron images (BSE) of samples #1–#4. The true identities of phases were all confirmed by analyzing the relevant XRD patterns shown in Fig. 2. The contents of Zn in the #2, #3 and #4 samples were rather higher than that in other alloys. Therefore, the liquid should present in the alloys at 500 °C. However, no amorphous phase was found in the XRD patterns, which means that the liquid phase has not been preserved after quenching. The phases determined from XRD were τ + (Zn) for the #4 sample indicating that the liquid phase transformed into (Zn) phase during cooling process. For the #2 and #3 samples, the compositions of the bright regions in Fig. 1(b) and (c) were at.% 24.6Al–75.4Zn and at.% 27.3Al–72.7Zn, respectively. The content of Al in the bright region exceeded the solid solution of Al in (Zn) and it was close to the composition of liquid at 500 °C. Therefore, it suggests that the liquid phase in the #2 and #3 samples transformed into (Al) + (Zn) phase during cooling process, which was concordant with the XRD results.

The phase constituent in the #1 sample measured from XRD was $TiAl_3$ + (Al). However, the Ti_2Al_5 (JCPDS 42–1134) was found to equilibrate with (Al) and (Zn) in the #2 sample. The compositions of the $TiAl_3$ in the #1 sample and Ti_2Al_5 in the #2 sample determined by EDS were at.% 26.6Ti–72.6Al–0.8Zn and at.% 26.2Ti–69.3Al–4.5Zn, respectively. According to the experimental results of Yang et al. [29], the $TiAl_3$ in the Al-rich corner was in stable equilibrium with (Al) and τ phases. However, the Ti_2Al_5 (JCPDS 42–1134) was in equilibrium with (Al) and τ phase at 400 °C observed in our previous experimental results [17]. The possible reason is that the solubility of Zn in Ti–Al alloys makes the Ti_2Al_5 more stable at 400 °C.

In order to verify the existence of Ti_2Al_5 in the Al-rich corner of the Al–Zn–Ti system, a single $Ti_{26}Al_{69}Zn_5$ alloy was prepared and its actual composition was at.% 27.7Ti–68.4Al–3.9Zn determined by ICP. Fig. 3 shows the XRD patterns of $TiAl_3$ and $Ti_{28}Al_{68}Zn_4$ powders. It can be seen that the major phase was $TiAl_3$ (JCPDS 65–4694) for $Ti_{25}Al_{75}$ alloy. However, no $TiAl_3$ was observed in $Ti_{28}Al_{68}Zn_4$ alloy and the major phases were Ti_2Al_5 (JCPDS 42–1134) and $TiAl_2$ (JCPDS 52–0861). After annealing at 500 °C for 5 days, the XRD pattern of $Ti_{28}Al_{68}Zn_4$ alloy has little change, which suggested that the Ti_2Al_5 phase can stably exist at 400 °C.

For the #3 and #4 samples, the phases determined from XRD were τ + (Al) + (Zn) and τ +(Zn), respectively. Single τ–$Ti_{27}Al_{28}Zn_{45}$ phase was found in the #5 sample, and the diffraction peaks were well consistent with that characteristic peaks determined in our previous work [16]. All the results were summarized and listed in Table 1. The chemical composition of each phase was averaged over at least three measurements of EDS.

5. Thermodynamic modeling and parameter optimization

In the present modeling, the thermodynamic parameters for the Al–Zn, Al–Ti and Zn–Ti systems are taken from Mey [18], Zhang et al. [19] and Luo et al. [26], respectively. In the following, the analytical expressions for the Gibbs energies of the ternary phases are presented briefly.

5.1. Solution phases

The liquid, (Al), hcp and bcc(Ti) are treated as solution phases. The Gibbs energy of a ternary solution phase is described by:

Table 1
Heat treatment conditions and experimental results of the Al–Zn–Ti system.

Samples	Actual composition (at.%)	Heat treatment	Phases by XRD	SEM and EDS			
				Phases	Composition (at.%)		
					Ti	Al	Zn
1#	Ti 11.4	500 °C/40 days	$TiAl_3$ + (Al)	$TiAl_3$	26.6	72.6	0.8
	Al 79.4			(Al)	0.4	83.9	15.7
	Zn 9.2						
2#	Ti 8.7	500 °C/40 days	Ti_2Al_5 + (Al) + (Zn)	Ti_2Al_5	26.2	69.3	4.5
	Al 67.1			(Al)		75.9	24.1
	Zn 24.2			Liquid		24.6	75.4
3#	Ti 15.4	500 °C/40 days	τ + (Al) + (Zn)	(Al)		74.9	25.1
	Al 55.7			τ	24.9	56.6	18.5
	Zn 28.9			Liquid		27.3	72.7
4#	Ti 16.2	500 °C/40 days	τ + (Zn)	τ	25.3	32.7	42.0
	Al 24.2			Liquid		6.5	93.5
	Zn 59.6						
5#	Ti 26.5	500 °C/40 days	τ	τ	24.7	26.3	48.9
	Al 28.5						
	Zn 45.0						

$$G^{\varphi} = x_{Al}G^{\circ,\varphi}_{Al} + x_{Zn}G^{\circ,\varphi}_{Zn} + x_{Ti}G^{\circ,\varphi}_{Ti} + RT(x_{Al}\ln x_{Al} + x_{Zn}\ln x_{Zn} + x_{Ti}\ln x_{Ti}) + x_{Al}x_{Zn}\sum_{k=0}^{m} {}^{k}L^{\varphi}_{(Al,Zn)}(x_{Al}-x_{Zn})^{k} + x_{Zn}x_{Ti}\sum_{k=0}^{m} {}^{k}L^{\varphi}_{(Zn,Ti)}(x_{Zn}-x_{Ti})^{k} + x_{Al}x_{Ti}\sum_{k=0}^{m} {}^{k}L^{\varphi}_{(Al,Ti)}(x_{Al}-x_{Ti})^{k} \quad (1)$$

where x_{Al}, x_{Zn} and x_{Ti} are the mole fractions of Al, Zn and Ti. The $G^{\circ,\varphi}_{Al}$, $G^{\circ,\varphi}_{Zn}$ and $G^{\circ,\varphi}_{Ti}$ denote the Gibbs energies of the pure Al, Zn and Ti with the φ structure. The ${}^{k}L^{\varphi}_{(Al,Zn)}$, ${}^{k}L^{\varphi}_{(Zn,Ti)}$ and ${}^{k}L^{\varphi}_{(Al,Ti)}$ are the binary interaction parameters.

5.2. Ternary ordered phases

Because of the solubility of Zn is about 0.8 at.% in $TiAl_3$ at 500 °C, the sublattice formula proposed for $TiAl_3$ phases is $(Ti,Al,Zn)_{0.25}(Al,Ti,Zn)_{0.75}$ by extending binary models of $(Ti,Al)_{0.25}(Al,Ti)_{0.75}$. The Gibbs energy per mole of the formula can be described by following expression

where y'_{Al}, y'_{Zn} and y'_{Ti} represent the site fractions of Al, Zn and Ti on the first sublattice, and y''_{Al}, y''_{Zn} and y''_{Ti} represent the site fractions of Al, Zn and Ti on the second sublattice. The parameter $G^{\varphi}_{Ti:Al}$ denotes the Gibbs energy of $Ti_{0.25}Al_{0.75}$. The terms ${}^{0}L_{Ti,Al:Al}$, ${}^{1}L_{Ti,Al:Al}$, ${}^{0}L_{Ti:Al,Ti}$ and ${}^{1}L_{Ti:Al,Ti}$ represent interaction parameters that are functions of temperature. For Ti_2Al_5, $TiAl_2$, TiZn and $TiZn_3$ phases, the sublattice formulas are $(Ti,Zn)_{0.33}(Al,Zn)_{0.67}$, $(Ti,Al)_{0.5}(Zn,Al)_{0.5}$ and $Ti_{0.25}(Zn,Al)_{0.75}$, respectively. Their Gibbs energy expressions are similar to Eq. (2).

The structure of the ternary phase τ has been determined as an $L1_2$ structure with Ti occupying (0, 0, 0) position and both Al and Zn occupying (0, 0.5, 0.5) position [16]. However, the previous HRXRD pattern and HRTEM results [16] suggest that a quantity of disorder phase exists in the alloy. According to the solubilities of Al, Zn and Ti in ternary phase τ phase [16,17,26,29], the τ phase is modeled as $(Ti)_{0.2}(Ti,Al,Zn)_{0.1}(Al,Zn)_{0.7}$, where $(Ti,Al,Zn)_{0.1}$ represents the miscible and disorder solubility of Al, Zn and Ti. Following expression gives the Gibbs energy of τ phase used in this study.

$$\begin{aligned} G^{TiAl_3} &= y'_{Ti}y''_{Al}G^{TiAl_3}_{Ti:Al} + y'_{Ti}y''_{Ti}G^{TiAl_3}_{Ti:Ti} + y'_{Ti}y''_{Zn}G^{TiAl_3}_{Ti:Zn} + y'_{Al}y''_{Al}G^{TiAl_3}_{Al:Al} + y'_{Al}y''_{Ti}G^{TiAl_3}_{Al:Ti} + y'_{Al}y''_{Zn}G^{TiAl_3}_{Al:Zn} \\ &+ y'_{Zn}y''_{Al}G^{TiAl_3}_{Zn:Al} + y'_{Zn}y''_{Ti}G^{TiAl_3}_{Zn:Ti} + y'_{Zn}y''_{Zn}G^{TiAl_3}_{Zn:Zn} + 0.25RT\left(y'_{Ti}\ln y'_{Ti} + y'_{Al}\ln y'_{Al} + y'_{Zn}\ln y'_{Zn}\right) + 0.75RT\left(y''_{Al}\ln y''_{Al} + y''_{Ti}\ln y''_{Ti} + y''_{Zn}\ln y''_{Zn}\right) \\ &+ y'_{Ti}y'_{Zn}y''_{Al}\,{}^{0}L^{TiAl_3}_{Ti,Zn:Al} + y'_{Ti}y''_{Al}y''_{Zn}\,{}^{0}L^{TiAl_3}_{Ti:Al,Zn} + y'_{Ti}y'_{Al}y''_{Al}\,{}^{0}L^{TiAl_3}_{Ti,Al:Al} + y'_{Ti}y'_{Al}y''_{Ti}L^{TiAl_3}_{Ti,Al:Ti} + y'_{Al}y''_{Al}y''_{Ti}\,{}^{0}L^{TiAl_3}_{Al:Al,Ti} + y'_{Ti}y''_{Al}y''_{Ti}\,{}^{0}L^{TiAl_3}_{Ti:Al,Ti} \end{aligned} \quad (2)$$

Table 2
The thermodynamic parameters of the Al–Zn–Ti system.

Phases	Models	Parameters	Ref.
Liquid	(Al,Zn,Ti)	${}^{0}L^{Liquid}_{Al,Zn} = 10465.55 - 3.9259T$	[18]
		${}^{0}L^{Liquid}_{Ti,Al} = -112,570 - 40.2529T$	[19]
		${}^{1}L^{Liquid}_{Ti,Al} = -7896.1$	[19]
		${}^{0}L^{Liquid}_{Ti,Zn} = -30,000 + 17.2T$	[26]
BCC(Ti)	(Al,Zn,Ti)	${}^{0}L^{BCC(Ti)}_{Ti,Al} = -125,485 + 36.8394T$	[19]
		${}^{0}L^{BCC(Ti)}_{Ti,Zn} = -50,700 + 32.5T$	[26]
HCP	(Al,Zn,Ti)	${}^{0}L^{HCP}_{Al,Zn} = 18820.95 + 8.95255T$	[18]
		${}^{3}L^{HCP}_{Al,Zn} = -702.79$	[18]
		${}^{0}L^{HCP}_{Ti,Al} = -123,789 + 33.209T$	[19]
		${}^{1}L^{HCP}_{Ti,Al} = -16034.9 + 12.1827T$	[19]
(Al)	(Al,Zn,Ti)	${}^{0}L^{(Al)}_{Al,Zn} = 7297.48 + 0.47512T$	[18]
		${}^{1}L^{(Al)}_{Al,Zn} = 6612.88 - 4.5911T$	[18]
		${}^{2}L^{(Al)}_{Al,Zn} = -3097.19 + 3.30635T$	[18]
		${}^{0}L^{(Al)}_{Ti,Al} = -124,270 + 43.8967T$	[19]
Ti_2Zn	$(Ti)_2(Zn)_1$	${}^{0}G^{Ti_2Zn}_{Ti:Zn} = 2G^{\circ,HCP}_{Ti} + G^{\circ,HCP}_{Zn} - 53499.9 + 22.2T$	[26]
Ti_3Zn_{22}	$(Ti)_{0.12}(Zn)_{0.88}$	${}^{0}G^{Ti_3Zn_{22}}_{Ti:Zn} = 0.12G^{\circ,HCP}_{Ti} + 0.88G^{\circ,HCP}_{Zn} - 11,170 + 4.5T$	[26]
$TiZn_{16}$	$(Ti)_1(Zn)_{16}$	${}^{0}G^{TiZn_{16}}_{Ti:Zn} = G^{\circ,HCP}_{Ti} + 16G^{\circ,HCP}_{Zn} - 109,310 + 54.4T$	[26]
$TiAl_2$	$(Ti,Zn)_1(Al,Zn)_2$	${}^{0}G^{TiAl_2}_{Ti:Al} = G^{\circ,FCC}_{Ti} + 2G^{\circ,FCC}_{Al} - 131575.2 + 33.0624T$	[19]
		${}^{0}G^{TiAl_2}_{Ti:Zn} = G^{\circ,HCP}_{Ti} + 2G^{\circ,HCP}_{Zn} - 47,250 + 21.39T$	This work
		${}^{0}G^{TiAl_2}_{Zn:Al} = G^{\circ,FCC}_{Zn} + 2G^{\circ,FCC}_{Al} + 15,000$	This work
		${}^{0}G^{TiAl_2}_{Zn:Zn} = 3G^{\circ,FCC}_{Zn}$	This work
Ti_3Al	$(Ti,Al)_{0.75}(Ti,Al)_{0.25}$	${}^{0}G^{Ti_3Al}_{Al:Al} = G^{\circ,HCP}_{Al}$	[19]
		${}^{0}G^{Ti_3Al}_{Ti:Al} = 0.75G^{\circ,HCP}_{Ti} + 0.25G^{\circ,HCP}_{Al} - 29633.6 + 6.70801T$	[19]
		${}^{0}G^{Ti_3Al}_{Al:Ti} = 0.75G^{\circ,HCP}_{Al} + 0.25G^{\circ,HCP}_{Ti} + 29633.6 - 6.70801T$	[19]
		${}^{0}G^{Ti_3Al}_{Ti:Ti} = G^{\circ,HCP}_{Ti}$	[19]

Table 2 (*continued*)

Phases	Models	Parameters	Ref.
		${}^{0}L^{Ti_3Al}_{Al,Ti:Al} = -71277.9 + 25.47T$	[19]
		${}^{0}L^{Ti_3Al}_{Al,Ti:Ti} = -71277.9 + 25.47T$	[19]
TiAl	$(Ti,Al)_{0.5}(Ti,Al)_{0.5}$	${}^{0}G^{TiAl}_{Al:Al} = G^{\circ,FCC}_{Al}$	[19]
		${}^{0}G^{TiAl}_{Ti:Al} = 0.5G^{\circ,FCC}_{Ti} + 0.5G^{\circ,FCC}_{Al} - 37445.1 + 16.7938T$	[19]
		${}^{0}G^{TiAl}_{Al:Ti} = 0.5G^{\circ,FCC}_{Al} + 0.5G^{\circ,FCC}_{Ti} + 37445.1 - 16.7938T$	[19]
		${}^{0}G^{TiAl}_{Ti:Ti} = G^{\circ,FCC}_{Ti}$	[19]
		${}^{0}L^{TiAl}_{Al,Ti:Al} = -63490.1 + 7.7928T$	[19]
		${}^{1}L^{TiAl}_{Al,Ti:Al} = 39488.4$	[19]
		${}^{0}L^{TiAl}_{Al,Ti:Ti} = -63490.1 + 7.7928T$	[19]
		${}^{1}L^{TiAl}_{Al,Ti:Ti} = -63490.1 + 7.7928T$	[19]
		${}^{0}L^{TiAl}_{Al:Al,Ti} = -28311.6 + 10.85167T$	[19]
		${}^{0}L^{TiAl}_{Ti:Al,Ti} = -28311.6 + 10.85167T$	[19]
TiZn	$(Ti,Al)_{0.5}(Zn,Al)_{0.5}$	${}^{0}G^{TiZn}_{Ti:Zn} = 0.5G^{\circ,HCP}_{Ti} + 0.5G^{\circ,HCP}_{Zn} - 20,900 + 7.75T$	[26]
		${}^{0}G^{TiZn}_{Ti:Al} = 0.5G^{\circ,HCP}_{Ti} + 0.5G^{\circ,FCC}_{Al} - 21445.1 + 16.79376T$	This work
		${}^{0}G^{TiZn}_{Al:Zn} = 0.5G^{\circ,FCC}_{Al} + 0.5G^{\circ,HCP}_{Zn}$	This work
		${}^{0}L^{TiZn}_{Ti:Al,Zn} = -17,000$	This work
		${}^{0}L^{TiZn}_{Ti,Al:Zn} = -27,000$	This work
$TiZn_2$	$(Ti,Al)_1(Zn,Al)_2$	${}^{0}G^{TiZn_2}_{Ti:Zn} = G^{\circ,HCP}_{Ti} + 2G^{\circ,HCP}_{Zn} - 62,250 + 21.39T$	[26]
$TiZn_3$	$(Ti)_{0.25}(Al,Zn)_{0.75}$	${}^{0}G^{TiZn_3}_{Ti:Zn} = 0.25G^{\circ,FCC}_{Ti} + 0.75G^{\circ,FCC}_{Zn} - 23327.365 + 8.7025T$	[26]
		${}^{0}G^{TiZn_3}_{Ti:Al} = 0.25G^{\circ,FCC}_{Ti} + 0.75G^{\circ,FCC}_{Al} - 20349.6 + 10.36525T$	This work
$TiAl_3$	$(Ti,Al,Zn)_{0.25}(Ti,Al,Zn)_{0.75}$	${}^{0}G^{TiAl_3}_{Al:Al} = G^{\circ,FCC}_{Al}$	[19]
		${}^{0}G^{TiAl_3}_{Ti:Al} = 0.25G^{\circ,FCC}_{Ti} + 0.75G^{\circ,FCC}_{Al} - 40349.6 + 10.3653T$	[19]
		${}^{0}G^{TiAl_3}_{Al:Ti} = 0.25G^{\circ,FCC}_{Al} + 0.75G^{\circ,FCC}_{Ti} + 40349.6 - 10.3653T$	[19]
		${}^{0}G^{TiAl_3}_{Ti:Ti} = G^{\circ,FCC}_{Ti}$	[19]
		${}^{0}G^{TiAl_3}_{Ti:Zn} = 0.25G^{\circ,FCC}_{Ti} + 0.75G^{\circ,FCC}_{Zn} - 6088.55 + 8.7025T$	This work
		${}^{0}G^{TiAl_3}_{Al:Zn} = 0.25G^{\circ,FCC}_{Al} + 0.75G^{\circ,FCC}_{Zn} + 6088.55 + 8.7025T$	This work
		${}^{0}G^{TiAl_3}_{Zn:Zn} = G^{\circ,FCC}_{Zn}$	This work
		${}^{0}G^{TiAl_3}_{Zn:Al} = 0.25G^{\circ,FCC}_{Zn} + 0.75G^{\circ,FCC}_{Al} + 5000$	This work
		${}^{0}L^{TiAl_3}_{Ti,Zn:Al} = -1150$	This work
		${}^{0}L^{TiAl_3}_{Ti:Al,Zn} = -33,414 + 18T$	This work
		${}^{0}L^{TiAl_3}_{Al,Ti:Al} = 12,500$	[19]
		${}^{0}L^{TiAl_3}_{Al,Ti:Ti} = 12,500$	[19]
		${}^{0}L^{TiAl_3}_{Al:Al,Ti} = -61849.5 + 36.5337T$	[19]
		${}^{0}L^{TiAl_3}_{Ti:Al,Ti} = -61849.5 + 36.5337T$	[19]
Ti_2Al_5	$(Ti,Zn)_{0.285714}(Al,Zn)_{0.714286}$	${}^{0}G^{Ti_2Al_5}_{Ti:Al} = 0.285714G^{\circ,FCC}_{Ti} + 0.714286G^{\circ,FCC}_{Al} - 40495.4 + 9.52964T$	[19]
		${}^{0}G^{Ti_2Al_5}_{Ti:Zn} = 0.285714G^{\circ,FCC}_{Ti} + 0.714286G^{\circ,FCC}_{Zn} + 36,300$	This work
		${}^{0}G^{Ti_2Al_5}_{Zn:Zn} = G^{\circ,FCC}_{Zn} + 40,000$	This work
		${}^{0}G^{Ti_2Al_5}_{Zn:Al} = 0.285714G^{\circ,FCC}_{Zn} + 0.714286G^{\circ,FCC}_{Al} + 30,025 + 25T$	This work
		${}^{0}L^{Ti_2Al_5}_{Ti:Al,Zn} = -55,000$	This work
		${}^{1}L^{Ti_2Al_5}_{Ti:Al,Zn} = -18,000$	This work
		${}^{0}L^{Ti_2Al_5}_{Ti,Zn:Al} = -15,700$	This work
		${}^{1}L^{Ti_2Al_5}_{Ti,Zn:Al} = -87,000$	This work
τ	$(Ti)_{0.2}(Ti,Al,Zn)_{0.1}(Al,Zn)_{0.7}$	${}^{0}G^{\tau}_{Ti:Ti:Al} = 0.3G^{\circ,FCC}_{Ti} + 0.7G^{\circ,FCC}_{Al} - 39088.55 + 9.9251T$	This work
		${}^{0}G^{\tau}_{Ti:Ti:Zn} = 0.3G^{\circ,FCC}_{Ti} + 0.7G^{\circ,FCC}_{Zn} - 22,800 + 8.7025T$	This work
		${}^{0}G^{\tau}_{Ti:Al:Al} = 0.2G^{\circ,FCC}_{Ti} + 0.8G^{\circ,FCC}_{Al} - 26908.55 + 9.9251T$	This work
		${}^{0}G^{\tau}_{Ti:Al:Zn} = 0.2G^{\circ,FCC}_{Ti} + 0.1G^{\circ,FCC}_{Al} + 0.7G^{\circ,FCC}_{Zn} - 22,600 + 8.7025T$	This work
		${}^{0}G^{\tau}_{Ti:Zn:Al} = 0.2G^{\circ,FCC}_{Ti} + 0.1G^{\circ,FCC}_{Zn} + 0.7G^{\circ,FCC}_{Al} - 29088.55 + 9.9251T$	This work
		${}^{0}G^{\tau}_{Ti:Zn:Zn} = 0.2G^{\circ,FCC}_{Ti} + 0.8G^{\circ,FCC}_{Zn} - 15,000 + 8.7025T$	This work
		${}^{0}L^{\tau}_{Ti:Al:Al,Zn} = -28300.79 + 10.5T$	This work
		${}^{1}L^{\tau}_{Ti:Al:Al,Zn} = 18001.31 - 7.429T$	This work
		${}^{0}L^{\tau}_{Ti:Zn:Al,Zn} = -28300.79 + 10.5T$	This work
		${}^{1}L^{\tau}_{Ti:Zn:Al,Zn} = 18001.31 - 7.429T$	This work
		${}^{0}L^{\tau}_{Ti:Ti:Al:Al} = -20,000$	This work
		${}^{0}L^{\tau}_{Ti:Ti:Al:Zn} = -5000$	This work
		${}^{0}L^{\tau}_{Ti:Ti:Al,Zn} = -20999.65$	This work

$$G^{\tau} = y'_{Ti}y''_{Al}y'''_{Al}G^{\tau}_{Ti:Ti:Al} + y'_{Ti}y''_{Al}y'''_{Al}G^{\tau}_{Ti:Al:Al} + y'_{Ti}y''_{Zn}y'''_{Al}G^{\tau}_{Ti:Zn:Al} + y'_{Ti}y''_{Ti}y'''_{Zn}G^{\tau}_{Ti:Ti:Zn} + y'_{Ti}y''_{Al}y'''_{Zn}G^{\tau}_{Ti:Al:Zn} + y'_{Ti}y''_{Zn}y'''_{Zn}G^{\tau}_{Ti:Zn:Zn}$$
$$+0.1RT\left(y''_{Ti}\ln y''_{Ti} + y''_{Al}\ln y''_{Al} + y''_{Zn}\ln y''_{Zn}\right) + 0.7RT\left(y'''_{Al}\ln y'''_{Al} + y'''_{Zn}\ln y'''_{Al}\right) + y'_{Ti}y''_{Al}y'''_{Al}y'''_{Zn}\left[{}^{0}L^{\tau}_{Ti:Al:Al,Zn} + {}^{1}L^{\tau}_{Ti:Al:Al,Zn}\left(y'''_{Al} - y'''_{Zn}\right)\right] \quad (3)$$
$$+y'_{Ti}y''_{Zn}y'''_{Al}y'''_{Zn}\left[{}^{0}L^{\tau}_{Ti:Zn:Al,Zn} + {}^{1}L^{\tau}_{Ti:Zn:Al,Zn}\left(y'''_{Al} - y'''_{Zn}\right)\right] + y'_{Ti}y''_{Ti}y''_{Al}y'''_{Al}{}^{0}L^{\tau}_{Ti:Ti,Al:Al} + y'_{Ti}y''_{Ti}y''_{Al}y'''_{Zn}{}^{0}L^{\tau}_{Ti:Ti,Al:Zn} + y'_{Ti}y''_{Ti}y'''_{Al}y'''_{Zn}{}^{0}L^{\tau}_{Ti:Ti,Al:Zn}$$

5.3. The assessment results of the Al–Zn–Ti system

The experimental data of phase equilibria at 400 °C [17] and 500 °C as well as the diffusion couple results at 400 °C [16] were used to assess the Al–Zn–Ti system. There were four obvious layers existed in the diffusion couple from pure Zn to $TiAl_3$. The diffusion path determined from the Zn/$TiAl_3$ diffusion couple were Zn (at.% 100Zn) → liquid (about at.% 5.8Al–94.2Zn) → τ (at.% 24.1Ti–57.0Al–18.9Zn) → $TiAl_3$ (at.% 27.1Ti–72.9Al). The Ti_2Al_5 phase was considered in this work because its existence has been confirmed. The parameters optimized in this work were listed in Table 2.

Fig. 4 is the calculated isothermal section of the Al-rich corner of the Al–Zn–Ti system at 400 °C. The experimental points [17] and the diffusion path are marked as red lines in Fig. 4. Fig. 5 shows the isothermal section of the Al-rich corner at 500 °C compared with the experimental data of this work. It can be seen that the calculated results agree well with experimental data except the #3 sample. The composition of the #3 sample (at.% 15.4Ti–55.7Al–28.9Zn) located in L + τ + Ti_2Al_5 phase region, but the XRD results showed that the phases were τ, (Al) and (Zn) in the #3 sample. The experimental phase composition of the #3 sample was also in conflict with that of the #2 sample which was consistent with the calculated phase region. Based on calculating the isoplethal section with 15.4 at.% Ti, it can be found that an invariant reaction, liquid + Ti_2Al_5 → τ + (Al), takes place at 499 °C. The phase equilibria in this field involving L, Ti_2Al_5, τ and (Al) have been changed above and below the invariant reaction temperature. The

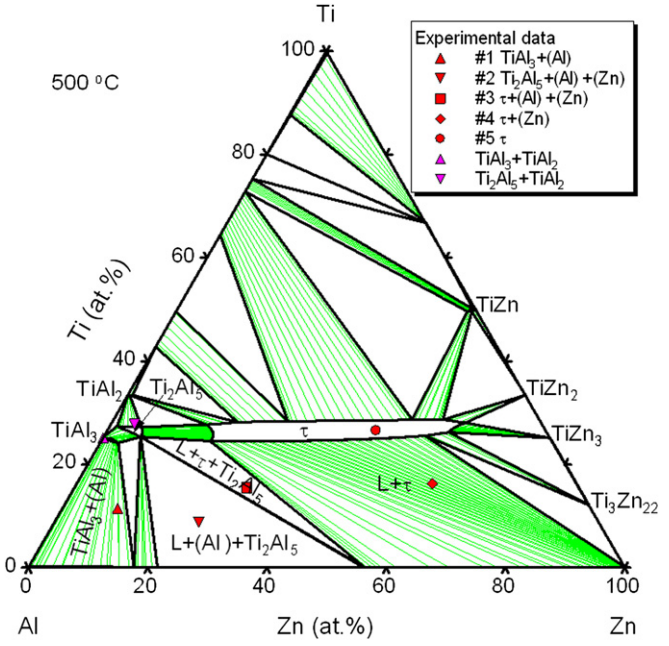

Fig. 5. The isothermal section of the Al-rich corner of the Al–Zn–Ti system at 500 °C.

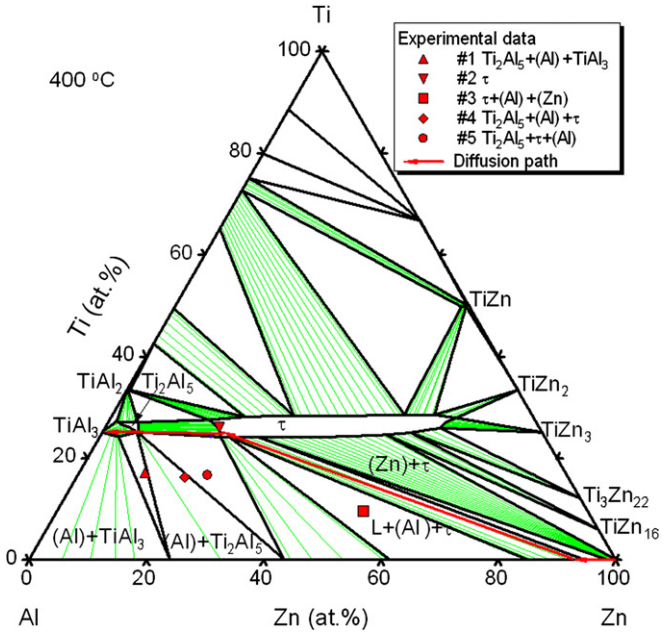

Fig. 4. The isothermal section of the Al-rich corner of the Al–Zn–Ti system at 400 °C.

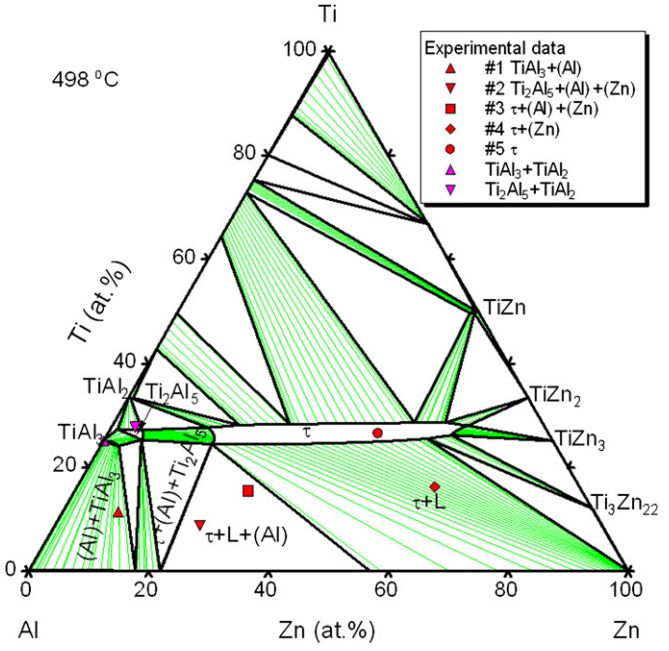

Fig. 6. The isothermal section of the Al-rich corner of the Al–Zn–Ti system at 498 °C.

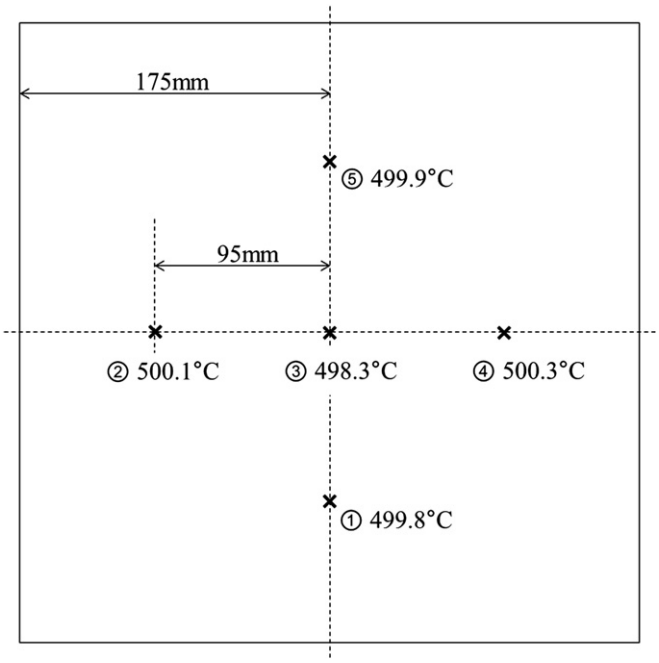

Fig. 7. The temperature profile in the furnace.

three phase equilibria showed in Fig. 5 were L + (Al) + Ti_2Al_5 and L + τ + Ti_2Al_5 at 500 °C. That were τ + (Al) + Ti_2Al_5 and τ + L + (Al) at 498 °C showed in Fig. 6. It is confirmed that the invariant reaction, liquid + Ti_2Al_5 → τ + (Al), happened between 498 and 500 °C. The measured phase composition of the #3 sample agreed with the calculated results at 498 °C (Fig. 6). It may be owing to the tiny temperature difference in different region of the chamber type electric resistance furnace. Therefore, the temperature profile in the furnace was measured and showed in Fig. 7 verified our estimation. Fig. 8 shows the plot of the calculated formation enthalpies of the $TiAl_3$–$TiZn_3$ intermediate phases at 27 °C with the experimental data reported by Delsante et al. [27], Meschel et al. [32] and Nassik [33], respectively. Good agreement has been reached between the calculated line and the experimental data.

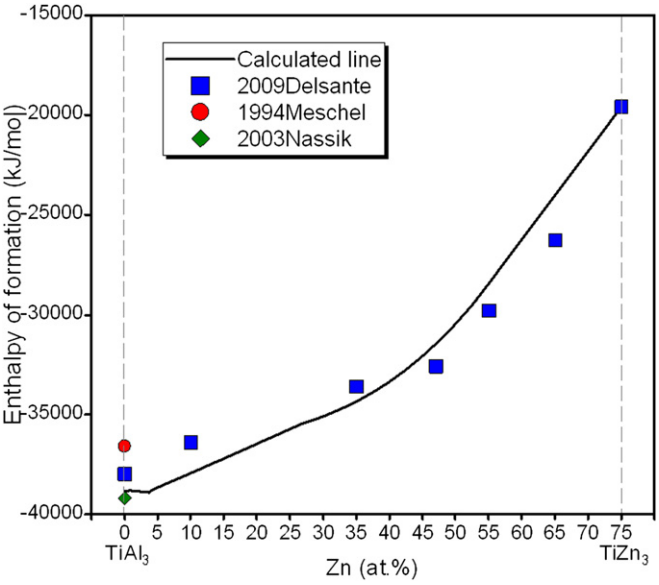

Fig. 8. The calculated enthalpy of formation of the $TiAl_3$–$TiZn_3$ intermediate phases at 27 °C. Square: [27], circle: [32], rhombus [33].

6. Conclusions

The Al-rich corner of the Al–Zn–Ti system has been experimentally and thermodynamically investigated. The results can be summarized as follows:

1. The phase relationships in the Al-rich corner of the Al–Zn–Ti system at 500 °C had been determined using equilibrated alloys approach by means of SEM, EDS and XRD. The phase with Ti_2Al_5 structure was identified in the Al-rich corner. The ternary phase τ is in equilibrium with $Ti_{26}Al_{69}Zn_5$, (Al) and liquid.
2. The existence of Ti_2Al_5 in the Al-rich corner prepared by sintered $Ti_{28}Al_{68}Zn_4$ powders has been confirmed by XRD. There is an obviously difference between the XRD patterns of Ti_2Al_5 and $TiAl_3$ phases. The reason of Ti_2Al_5 being stable at 400 °C might be that the solubility of Zn in the Ti–Al alloy leads to its structure change.
3. The self-consistent thermodynamic description was obtained by assessing our experimental data and information from literatures. The calculated isothermal sections in the Al-rich corner and the calculated formation enthalpies of the $Ti_{25}Zn_xAl_{75-x}$ (x = 0–75) alloys agreed well with the experimental data.

Acknowledgments

The authors thank Instrumental Analysis and Research Center of Shanghai University for their support of materials testing and research. This work was financially supported by the National Natural Science Foundation of China (50974084), Chinese National Key Technology R&D Program (2007BAE09B03), Guizhou Province (Key Science and Technology Development Program in the Eleventh Five-Year Plan, 20076003) and Aluminum Corporation of China (Science and Technology Development Fund, 2007KJA07).

References

[1] Chou CY, Lee SL, Lin JC, Hsu CM. Effect of cross-channel extrusion on the microstructures and superplasticity of a Zn–22 wt.% Al eutectoid alloy. Scripta Mater 2007;57:972–5.
[2] Kawasaki M, Langdon TG. Developing superplasticity and a deformation mechanism map for the Zn–Al eutectoid alloy processed by high-pressure torsion. Mater Sci Eng A 2011;528:6140–5.
[3] Xia SH, Wang J, Wang JT, Liu JQ. Improvement of room-temperature superplasticity in Zn–22 wt.% Al alloy. Mater Sci Eng A 2008;493:111–5.
[4] Tanaka T, Takigawa Y, Higashi K. Effect of temperature on the cavity nucleation rate for fine-grained Zn–22 wt.% Al alloy. Scripta Mater 2008;58:643–6.
[5] Hirata T, Tanaka T, Chung SW, Takigawa Y, Higashi K. Relationship between deformation behavior and microstructural evolution of friction stir processed Zn–22 wt.% Al alloy. Scripta Mater 2007;56:477–80.
[6] Tanaka T, Kohzu M, Takigawa Y, Higashi K. Low cycle fatigue behavior of Zn–22 mass% Al alloy exhibiting high-strain-rate superplasticity at room temperature. Scripta Mater 2005;52:231–6.
[7] Honda K, Sugiyama M, Ikematsu YY, Ushioda K. Role of $TiAl_3$ fine precipitate in nucleation of the primary Al dendrite phase during solidification in hot-dip Zn–11%Al–3%Mg–0.2%Si coated steel sheet. Mater Trans 2011;52:90–5.
[8] Honda K, Ushioda K, Yamada W. Nucleation of the primary Al phase on $TiAl_3$ during solidification of a hot-dip Zn–11%Al–3%Mg–0.2%Si coating on steel sheet. Ceram Trans 2009;201:355–62.
[9] Honda K, Ushioda K, Yamada W. Mechanism on heterogeneous nucleation of the primary Al phase on $TiAl_3$ of a hot-dip Zn–11%Al–3%Mg–0.2%Si coating on steel sheet. Mater Sci Forum 2010;638–642:2787–92.
[10] Seidman DN, Marquis EA, Dunand DC. Precipitation strengthening at ambient and elevated temperatures of heat-treatable Al(Sc) alloys. Acta Mater 2002;50:4021–35.
[11] Pourkia N, Emamy M, Farhangi H, Seyed Ebrahimi SH. The effect of Ti and Zr elements and cooling rate on the microstructure and tensile properties of a new developed super high-strength aluminum alloy. Mater Sci Eng A 2010;527:5318–25.

[12] Krajewski WK, Buras J, Zurakowski M, Greer AL, Mancheva MN, Haberl K, et al. Development of environmentally friendly cast alloys. High-zinc Al alloys. Arch Mater Sci Eng A 2010;45:120–4.
[13] Ai XL, Quan GF, Yang J, Liu ZM. Effect of Ti addition on the microstructure and mechanical properties of cast AZ91 magnesium alloy. Adv Mat Res 2011;189–193:3819–23.
[14] Zhang MX, Kelly PM, Easton MA, Taylor JA. Crystallographic study of grain refinement in aluminum alloys using the edge-to-edge matching model. Acta Mater 2005;53:1427–38.
[15] Iqbal N, van Dijk NH, Offerman SE, Moret MP, Katgerman L. Real-time observation of grain nucleation and growth during solidification of aluminum alloys. Acta Mater 2005;53:2875–80.
[16] Luo Q, Li Q, Jin F, Zhang JY, Yu XB, Gu QF, et al. The crystal structure, microhardness and thermal stability of the $Ti_{26}Al_{55}Zn_{19}$ alloy. Intermetallics 2012;26:136–41.
[17] Luo Q, Jin F, Li Y, Li Q, Zhang JY, Chou KC. Experimental investigation of the phase equilibria of Al–Zn–Ti system in Al-rich corner at 400 °C. Adv Mater Res 2012;399–401:2210–4.
[18] Mey SA. Reevaluation of the Al–Zn system. Z Metallkd 1993;84:451–5.
[19] Zhang F, Chen SL, Chang YA, Kattner UR. A thermodynamic description of the Ti–Al system. Intermetallics 1997;5:471–82.
[20] Murray JL. The Ti–Zn (titanium–zinc) system. Bull Alloy Phase Diagr 1984;5:52–6.
[21] Vassilev GP, Liu XJ, Ishida K. Reaction kinetics and phase diagram studies in the Ti–Zn system. J Alloy Compd 2004;375:162–70.
[22] Chen XA, Jeitschko W, Danebrock ME, Evers CBH, Wagner K. Preparation, properties, and crystal structures of Ti_3Zn_{22} and $TiZn_{16}$. J Solid State Chem 1995;118:219–26.
[23] Ghosh G, Delsante S, Botzone G, Asta M, Ferro R. Phase stability and cohesive properties of Ti–Zn intermetallics: first-principles calculations and experimental results. Acta Mater 2006;54:4977–97.
[24] Anderson EA, Boyle EJ, Ramsey PW. Rolled zinc–titanium alloys. Trans AIME 1944;156:278–86.
[25] Saillard M, Develey G, Becle C, Moreau JM, Paccard D. The structure of $TiZn_{16}$. Acta Crystallogr 1981;B37:224–6.
[26] Luo Q, Li Q, Zhang JY, Chen SL, Chou KC. A thermodynamic description of the Al–Zn–Ti ternary system. In: The 15th national conference of phase diagram of China and multilateral symposium on phase diagrams and materials design, 2010, Shenyang.
[27] Delsante S, Ghosh G, Borzone G. A calorimetric study of alloys along the $Ti(Al, Zn)_3$ section. Calphad 2009;33:50–4.
[28] Doi K, Ono S, Ohtani H, Hasebe M. Thermodynamic study of the phase equilibria in the Sn–Ti–Zn ternary system. J Phase Equilib Diff 2006;27:63–74.
[29] Yang S, Su XP, Wang JH, Yin FC, Li Z, Tu H, et al. The Zn-rich corner of the Zn–Al–Ti system at 723 K. J Alloy Compd 2010;499:194–9.
[30] Raman A, Schubert K. Uber den aufbau einiger zu $TiAl_3$ verwandter legierungsreihen. I. Untersuchungen in einigen T4–Zn–Al–, T4–Zn–Ga– und T4–Ga–Ge–systemen. Z Metallkde 1965;56:40–3.
[31] Krajewski WK. Determination of Al site preference in $L1_2$ $TiZn_3$-base trialuminides. Mater Sci Forum 2006;508:615–20.
[32] Meschel SV, Kleppa OJ. In: Faulkner JS, Jordan RG, editors. Metallic alloys: experimental and theoretical perspectives. Dordrecht: Kluwer; 1994. p. 103.
[33] Nassik M, Chrifi-Alaoui FZ, Mahdouk K, Gachon JC. Calorimetric study of the aluminium–titanium system. J Alloys Compd 2003;350:151–4.